Phase diagram for the antiferromagnetic Blume-Capel model near tricriticality

J. D. Kimel
Department of Physics B-159 and Supercomputer Computations Research Institute B-186, Florida State University, Tallahassee, Florida 32306

Per Arne Rikvold
Department of Physics B-159 and Supercomputer Computations Research Institute B-186 and Center for Materials Research and Technology B-159, Florida State University, Tallahassee, Florida 32306 and Tohwa Institute for Science, Tohwa University, Fukuoka 815, Japan*

Yung-Li Wang
Department of Physics B-159 and Supercomputer Computations Research Institute B-186 and Center for Materials Research and Technology B-159, Florida State University, Tallahassee, Florida 32306
(Received 14 August 1991)

We study the two-dimensional, antiferromagnetic Blume-Capel model on a square lattice by numerical transfer-matrix and Monte Carlo finite-size scaling methods, in order to investigate whether the line of tricritical points in this model may be decomposed into lines of critical end points and double critical points, as predicted by mean-field theory and recent Monte Carlo simulations on a three-dimensional cubic lattice. Conclusive numerical evidence is obtained, indicating that such decomposition does *not* occur in this two-dimensional model. The nondecomposition is explained in terms of the large fluctuations in the two-dimensional nearest-neighbor model, and we speculate that the situation may be different in two-dimensional antiferromagnetic models with weak, ferromagnetic next-nearest-neighbor interactions.

I. INTRODUCTION

The Blume-Capel model[1,2] and its generalization, the Blume-Emery-Griffiths[3] or $S=1$ Ising model, which is equivalent to a three-state lattice-gas model,[4] have been extensively studied. As discussed in Ref. 5, the strong interest in these models arises partly from the unusually rich phase-transition behavior they display as their interaction parameters are varied, and partly from their many possible applications.

One of the most interesting and elusive features of the mean-field phase diagram for the antiferromagnetic Blume-Capel model in an external field is the decomposition of a line of tricritical points into a line of critical end points and one of double critical points.[6] A similar decomposition is predicted by mean-field theory for anisotropic magnetic models with ferromagnetic intrasublattice and antiferromagnetic intersublattice interactions.[7] However, a Monte Carlo renormalization-group study was unable to confirm this prediction unequivocally, although the effective critical exponents obtained indicated that the decomposition may be taking place in three dimensions.[8] Other examples are provided by the Blume-Emery-Griffiths model with repulsive biquadratic coupling,[9] and an $S=\frac{1}{2}$ Ising model in a trimodally distributed random field.[10] (A number of different names are used in the literature to describe the double critical point, including "double critical end point" or "bicritical end point,"[8] and "ordered critical point."[10]) A clear numerical confirmation of this decomposition phenomenon was obtained by two of us in a recent Monte Carlo simulation of the Blume-Capel model on a three-dimensional cubic lattice.[11] In contrast, for the two-dimensional square lattice the results of our previous Monte Carlo simulations[12] are (i) no evidence for the decomposition of the tricritical points is seen and, (ii) the second-order line persists around the region of high curvature near the tricritical point, whereas the mean-field calculation had the first-order line extending around the promontory. Analogous results have also been obtained in transfer-matrix studies of Blume-Emery-Griffiths models on a triangular lattice.[5,13]

The main purpose of the present paper is to examine, for the antiferromagnetic Blume-Capel model, whether these qualitative differences between the two-dimensional Monte Carlo simulations on the one hand, and the mean-field approximation and three-dimensional Monte Carlo simulation on the other, are supported by further Monte Carlo simulations and numerical transfer-matrix finite-size scaling (TMFSS) calculations in two dimensions. In order to verify the consistency of the Monte Carlo and transfer-matrix methods, we use finite-size scaling extrapolations, both for the Monte Carlo and transfer-matrix data. Our results reconfirm the nondecomposition of the tricritical points and the migration of the location (compared to the mean-field theory prediction) of the tricritical points for the two-dimensional case. In the course of our discussion we also present global phase diagrams, which require a large number of data points that are economically obtained by the TMFSS method.[5,13,14]

The remainder of this paper is organized as follows: In

Sec. II we give the Hamiltonian which defines the model, discuss the ground-state diagram, and briefly present the global, finite-temperature phase diagrams obtained by the TMFSS method. This method is discussed in Sec. III, and the Monte Carlo method and relevant finite-size scaling relations in Sec. IV. Our numerical results are presented in detail in Sec. V, and Sec. VI contains a summary and a discussion of the physical reasons for the marked differences between the two-dimensional system on the one hand, and the three-dimensional system and mean-field approximation on the other, as well as some suggestions for future work.

II. MODEL AND GLOBAL PHASE DIAGRAMS

The Hamiltonian for the antiferromagnetic Blume-Capel model is given by[6,12]

$$\mathcal{H}=-J\sum_{\langle i,j\rangle}s_i s_j+D\sum_i s_i^2-H\sum_i s_i \ . \tag{1}$$

Here the local spin variables are $s_i\in\{-1,0,+1\}$, the spin-spin interactions are antiferromagnetic ($J<0$), the field D distinguishes only between zero and nonzero values of the s_i, and the field H is a standard Ising magnetic field. The summations $\sum_{\langle i,j\rangle}$ are taken over all nearest-neighbor pairs, and $\sum_i$ over all sites of a square lattice. The Hamiltonian and phase diagrams are invariant under the transformation ($H\rightarrow -H$, $s_i\rightarrow -s_i$).

The corresponding ground-state diagram for the antiferromagnetic Blume-Capel model on a square lattice is shown in Fig. 1. It is obtained by identifying the ordered phases that can be reached via a continuous phase transition from a disordered phase, and pairwise equating the energies of the different phases. The detailed procedure, as applied to a general $S=1$ Ising model on a triangular lattice, is described in Refs. 5 and 14. The group-theoretical arguments involved are discussed in Refs. 15 and 16. There are three ordered ground states with antiferromagnetic symmetry. Referring to the sublattice magnetizations, we denote these states $(0-)$, $(+-)$, and $(+0)$, respectively. The three uniform ground states are analogously termed $(--)$, (00), and $(++)$. In the asymptotic limit of large negative D, the model becomes equivalent to the $S=\frac{1}{2}$ Ising model with effective interactions J and effective field H. In the limit of $(\pm H+D)>>|J|$ and $\pm H>0$, it becomes equivalent to $S=\frac{1}{2}$ Ising models with effective interactions $\frac{1}{4}J$ and effective fields $\frac{1}{2}(\pm H-D)+J$, when Eq. (1) is rewritten in terms of spin variables $\sigma_i\in\{-1,+1\}$.

Global views of the transition surface, which are qualitatively similar to those presented in previous mean-field[17] and Monte Carlo[12] studies, are presented in Figs. 2(a) and 2(b). The TMFSS method by which these global

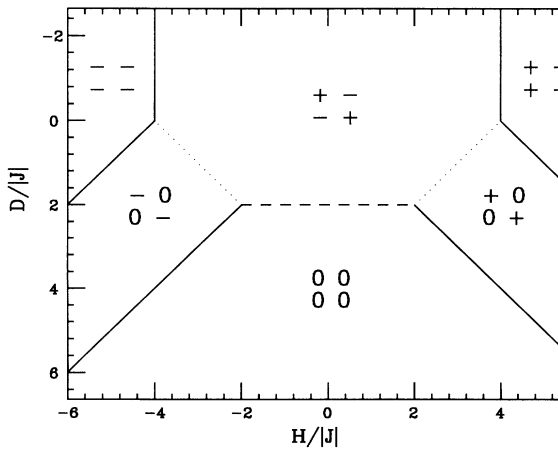

FIG. 1. Ground-state diagram for the square-lattice Blume-Capel model. The solid lines represent transitions which are second-order at nonzero T, whereas the dashed line corresponds to transitions which are first-order at low nonzero T. The dotted lines represent order-order transitions which are absent at nonzero T, due to the lack of next-nearest-neighbor interactions. The configurations corresponding to the different phases are also shown. Each configuration is illustrated on a 2×2 block of the lattice, which contains two sites from each sublattice. See detailed discussion in the text.

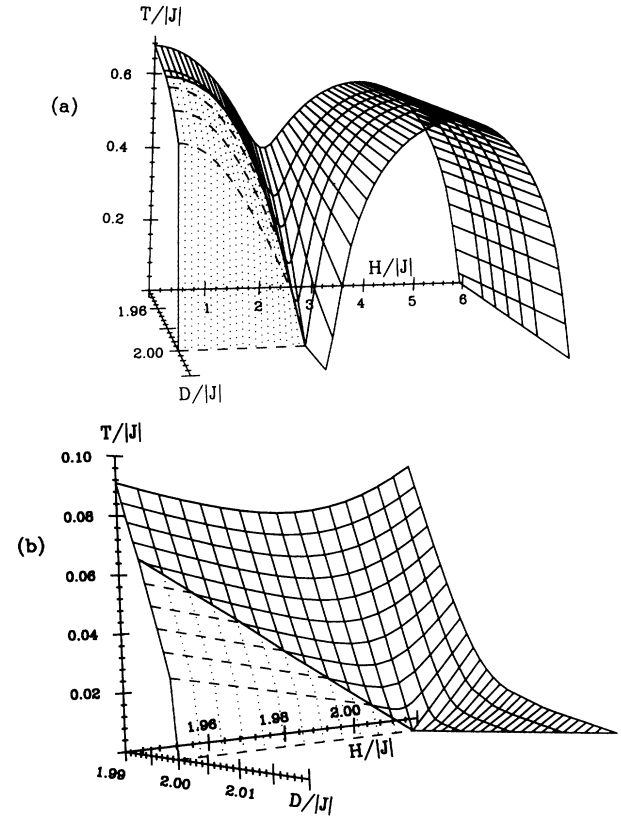

FIG. 2. Global (D,H,T) phase diagram, based on transfer-matrix calculations with $M'/M=4/6$. The view is in the direction of the negative D axis, with the positive H axis pointing to the right, and corresponds to the orientation of the ground-state diagram in Fig. 1. The surface of second-order transitions is indicated by solid lines at constant D and H. The surface of first-order transitions, which separates the ordered phase $(+-)$ from the disordered phase (00) at low $T/|J|$, is indicated by dashed lines at constant D and dotted lines at constant H. The two surfaces join smoothly along a line of tricritical points. (a) View of the entire surface for $H\geq 0$ and $1.94\leq D/|J|\leq 2.02$. Note the very different scales on the three axes. (b) Magnified detail of the surface near the point $H/|J|=D/|J|=2$, $T=0$. See detailed discussion in the text.

phase diagrams were obtained, is discussed in Sec. III, and the detailed numerical results are presented in Sec. V. Due to the absence of next-nearest-neighbor interactions, there are no order-order transitions separating the ordered phases, even at low nonzero temperatures. In the equivalent lattice-gas model this effect is easily understood as the result of each site on one sublattice being isolated within a "cage" of occupied sites on the other sublattice.[5] The ordered and disordered phases are separated by a surface of order-disorder transitions at nonzero temperatures. This surface mostly consists of second-order transitions in the Ising universality class, except for the portion at low T and $D>0$, whose intersection with the $T=0$ plane is shown as a dashed line in Fig. 1. It is the detailed topology of this transition surface which is under study in the present paper, with particular emphasis on determining whether the first- and second-order surfaces are joined along a line of tricritical points, or whether this line is decomposed into a line of critical end points and one of double critical points, as predicted by mean-field theory.

III. TRANSFER-MATRIX FINITE-SIZE SCALING CALCULATIONS

In the usual fashion,[18–20] infinitely long, strip-shaped systems of finite width M were partitioned into transverse layers parallel to one of the primitive lattice vectors. The full $3^M\times 3^M$ transfer matrix, which is symmetric, was block diagonalized utilizing invariance under one-step translations in the transverse direction. The symmetric and antisymmetric blocks, $\mathbf{T}^{\mathbf{S}}$ (834×834 for $M=8$) and $\mathbf{T}^{\mathbf{A}}$ (831×831 for $M=8$), are the only two blocks whose symmetries correspond to the ordered phases. They are both symmetric under matrix transposition, and were numerically diagonalized with the EISPACK routine RS on a Cyber 205 supercomputer at Florida State University. The eigenvalues, λ_α^S and λ_α^A, are numbered by the subscript α in order of decreasing norm. The overall dominant eigenvalue, λ_1^S, is known to be positive and nondegenerate by the Perron-Frobenius theorem.

Second-order phase transitions were located by the linear divergence with M of the overall dominant length scale, $\xi_1^A=(\ln|\lambda_1^S/\lambda_1^A|)^{-1}$, according to the Nightingale finite-size scaling criterion.[18–20] This length is microscopic in the disordered phase and diverges exponentially with M in all the ordered phases. The overall second largest length (the persistence length) is $\xi_1^S=(\ln|\lambda_1^S/\lambda_2^S|)^{-1}$. It remains small and independent of M in both the ordered and in the disordered phases, but peaks narrowly near the phase transitions. The tricritical line was located by the linear divergence of ξ_1^S with M. This scaling method for determining tricritical points in $S=\frac{1}{2}$ Ising models has been discussed in Refs. 21–27, and in Ref. 5, 13, and 14 it was successfully applied to a three-state lattice-gas model on a triangular lattice. In those regions of the (D,H,T) space where ξ_1^S diverges faster than linearly with M, the first-order transitions were accurately located by the equality of the matrix elements with the eigenvectors corresponding to the two largest eigenvalues of $\mathbf{T}^{\mathbf{S}}$ of the operator corresponding to $\langle s_i^2\rangle$. This criterion corresponds to the exchange of stability characteristic of a first-order transition.[5,13,14,24,27] Finite-size scaling estimates for the critical exponent ν were obtained by a generalization to two fields of the differentiation-free algorithm presented in Ref. 28. The exponent η was obtained from the scaling relation $\eta_M=M/[\pi\xi_1^A(M)]$,[29] which requires conformal invariance.[30–32]

Due to nonsingular contributions and corrections to scaling, the critical temperatures T_M obtained by using the Nightingale criterion with two strip widths, M' and M, do not equal the exact infinite system T_∞, but rather converge toward it according to a power law

$$T_M=T_\infty+CM^{-\omega}\ , \tag{2}$$

where the exponent ω depends on the subdominant critical exponents.[33–36] Since ω is not known, we here estimate T_∞ from a three-point power-law fit by numerically solving the equation

$$\left[\frac{T_4-T_\infty}{T_6-T_\infty}\right]^{\ln(6/8)}=\left[\frac{T_6-T_\infty}{T_8-T_\infty}\right]^{\ln(4/6)}\ , \tag{3}$$

for T_∞. Analogous extrapolations can be performed for other quantities, such as the critical exponents, but for the small system sizes used here the resulting estimates are not always accurate, mainly due to wrap-around effects for $M'=2$.

IV. MONTE CARLO SIMULATION AND FINITE-SIZE SCALING

The systems studied were $L\times L$ square lattices with even L and periodic boundary conditions, containing $N=L^2$ spins. The spin configurations were updated according to a highly vectorized two-sublattice checkerboard Metropolis[37] algorithm, visiting each lattice site sequentially once to complete one Monte Carlo step per spin (MCS). The simulations were performed on the Cyber 205 and ETA 10 supercomputers at Florida State University. In each simulation run an initial 2000–5000 MCS were allowed for thermal equilibration, depending on the phase point under study. The expectation value of the physical quantity O was estimated by

$$\langle O\rangle=\frac{1}{S}\sum_{c=1}^{S}O(c)\ , \tag{4}$$

where S is the total number of MCS in the run, following equilibration, and the index c is incremented once per MCS.

The relevant low-temperature antiferromagnetic order parameter is the staggered magnetization,

$$M_s(c)=\frac{1}{N}\sum_i\delta_i s_i(c)\ , \tag{5}$$

where i runs over the lattice sites and $\delta_i=+1$ ($\delta_i=-1$) for sites on the even (odd) sublattice, respectively. Its expectation value was estimated from Eq. (4) with $O(c)=|M_s(c)|$. We also calculated the staggered magnetic susceptibility,

$$\chi_s = (N/T)(\langle M_s^2 \rangle - \langle |M_s| \rangle^2) , \quad (6)$$

which is proportional to the variance in the order parameter. (We use units in which Boltzmann's constant is set to unity.) To obtain reliable error estimates in the Monte Carlo simulation, we used the binning method, described, for example, in Ref. 38.

Finite-size scaling[39,40] has been reviewed in general terms elsewhere,[33,41] as well as with particular emphasis on Monte Carlo simulations,[42,43] and will merely be applied here. The antiferromagnetic Blume-Capel model on a two dimensional lattice is expected to be in the universality class of the two-dimensional Ising model,[44] with critical exponents $\beta = \frac{1}{8}$, $\gamma = \frac{7}{4}$, and $\nu = 1$.[45,46] Thus, if T_∞ and T_L represent the transition temperatures for the bulk ($L \to \infty$) and finite lattice, respectively, we expect,[42,43] as $L \to \infty$,

$$(T_L - T_\infty)/T_\infty \sim L^{-1/\nu} , \quad (7)$$

with $\nu = 1$. As in Ref. 12, T_L was located by the maximum of χ_s, and the infinite-lattice transition temperature T_∞ was estimated by fitting T_L to

$$T_L = T_\infty + CL^{-1} , \quad (8)$$

using the linear least-squares method.

V. RESULTS

The global (D,H,T) phase diagram, based on transfer-matrix calculations with $M'/M = 4/6$, is shown in Figs. 2(a) and 2(b). Although these results contain non-negligible finite-size effects in certain regions of the phase diagram, they present a qualitatively and semiquantitatively correct picture which, for the two-dimensional model, is superior to that obtainable by mean-field calculations. More precise assessments of the finite-size effects are given below. Figure 2(a) shows a view of the surface of phase transitions for $H \geq 0$ and $1.94 \leq D \leq 2.02$. It consists of two "tunnels" of second-order transitions. The one parallel to the direction $H = D$ represents the transition to the ordered phase (+0), whereas the one parallel to the negative D axis represents the transition to the ordered phase (+ −). At low temperatures the latter phase is separated from the disordered phase (00) by a surface of first-order transitions, which is joined to the surface of second-order transitions as discussed at the end of Sec. II. In Fig. 2(b) is shown a magnified portion of the phase diagram, where the surfaces of second-order and first-order transitions merge near the point $H/|J| = D/|J| = 2, T = 0$. On this scale the first- and second-order surfaces are seen to join smoothly along a line of tricritical points which is almost straight and shows no signs of decomposition. These results agree with those of our Monte Carlo simulations, and provide further evidence that no decomposition of the tricritical line occurs, in contrast to the mean-field results and the three-dimensional case.[6,11,12]

To settle fully the issue of whether or not the tricritical line decomposes in two dimensions, we have also performed transfer-matrix calculations with $M'/M = 6/8$ at $D/|J| = 1.94$ and 1.98. The choice $D/|J| = 1.98$ corresponds to the value chosen for the Monte Carlo simulations in Ref. 12. For this value of D, the temperature at which the first- and second-order transition surfaces come together is sufficiently high to allow convergence of our Monte Carlo and transfer-matrix algorithms. The value $D/|J| = 1.94$ represents a nearby plane in the phase diagram, in which no first-order transitions occur. These results are included in Fig. 3, together with additional Monte Carlo data for $L = 32$ and 40. The locations of the second-order transition points were determined in the Monte Carlo simulation by the maxima of the staggered magnetic susceptibility. The first-order line was determined using a mixed start technique in which the upper half of the lattice was initialized to the $T = 0$ configuration expected on one side of the first-order boundary, i.e., (+ −), and the lower half plane initialized to the configuration expected on the other side of the first-order boundary, (00). By monitoring the

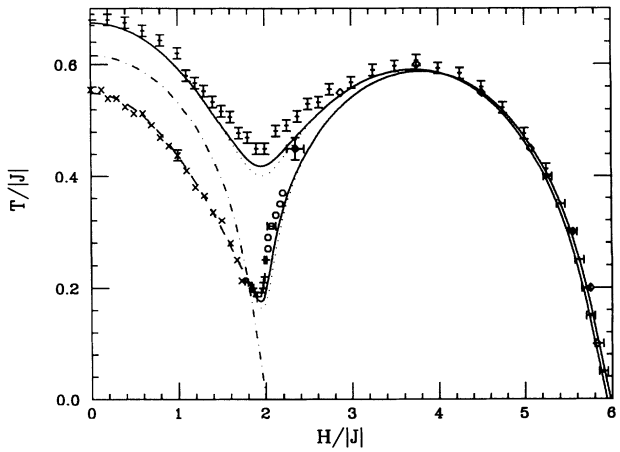

FIG. 3. Sections of the phase diagram for $D/|J| = 1.94$ and 1.98. For $D/|J| = 1.94$, Monte Carlo results are included for $L = 32$ with 12 000 MCS (+ with error bars). For the second-order line at $D/|J| = 1.98$, Monte Carlo results are included for $L = 40$ with 50 000 to 150 000 MCS (+); $L = 40$ with 8000 MCS (○); $L = 40$ with 1500 MCS (◇); and for the first-order line $L = 32$ mixed start algorithm (×). Error bars are shown only for representative points at $D/|J| = 1.98$. The TMFSS results for the second-order transitions were obtained with $M'/M = 4/6$, except in the interval $1.7 \leq H/|J| \leq 2.3$, where $M'/M = 6/8$ was used (solid lines). (The results obtained with $M'/M = 4/6$ are shown throughout as dotted lines to indicate the size of the finite-size effects.) The line of first-order transitions at $D/|J| = 1.98$ (dashed line, partly hidden behind the Monte Carlo points ×) was obtained with $M = 6$, as described in Sec. III. The dot-dashed line is the projection onto the H,T plane of the tricritical line obtained with $M'/M = 4/6$. The agreement between the Monte Carlo and transfer-matrix results is excellent, neither method showing any evidence for decomposition of the tricritical point, and both agreeing within errors on the location of the tricritical point. The apparent disagreement in the region $1.7 \leq H/|J| \leq 3$ is due to finite-size effects and can be virtually eliminated by finite-size scaling extrapolations, as discussed in the text and shown in Fig. 4.

configuration of the lattice after each update sweep, we were able to determine which of the two configurations the lattice tended toward, and thus on which side of the first-order line the system was located. By iterating this procedure, the Monte Carlo results for the first-order line shown in Fig. 3 were obtained. The consistency between the transfer-matrix and Monte Carlo results is indeed satisfying and confirms the correctness of the nonperturbative results, *vis à vis* the mean-field calculation. In particular, the results of the two approaches practically overlap in the regions of the first-order phase transition and close to the tricritical point, as well as for $H/|J|>3$. The differences that remain in the region where the transition line is strongly curved are due to finite-size effects and can be eliminated within statistical errors, using finite-size scaling as discussed below.

Due to corrections to scaling, the transfer-matrix data are expected to approach the infinite-system limit as a power law with an exponent which is a function of the subdominant critical exponents, as discussed in Sec. III.[33–36] The extrapolated transfer-matrix results are shown in Fig. 4 (which represents a close-up of Fig. 3 in the interval $1.7 \leq H/|J| \leq 2.3$) together with the finite-size results for $M'/M=2/4$, $4/6$, and $6/8$. The finite-size effects are substantial in the regions where the critical surface is strongly curved, but the extrapolations nevertheless converge to estimates that agree closely with the extrapolated Monte Carlo results, as discussed below. Near the first-order region the finite-size effects are small, and the extrapolated second-order line joins the first-order line smoothly without any discernible discontinuity in slope. We take this as further evidence that the line along which the first- and second-order transition surfaces meet is, indeed, a line of undecomposed tricritical points.

The finite-size Monte Carlo estimates for the critical temperatures T_L are those temperatures for which the staggered susceptibility has its maximum. These estimates converge towards the infinite-system limit as L^{-1}, as expected from Eq. (7) with $\nu=1$. The extrapolated Monte Carlo results shown in Fig. 4 were obtained from simulations for $L=20$, 26, 34, 48, and 100, except for $D/|J|=1.94$ and $H/|J|=2.00$, for which a simulation with $L=200$ was also included. The lengths of the simulations varied from $S=50\,000$ to $200\,000$ MCS, depending on the correlation time (in MCS) of the simulation at the particular point in parameter space. In each instance the simulated data points were consistent with the linear behavior in $1/L$, in agreement with Eq. (8). The extrapolated results of the Monte Carlo simulations are summarized in Table I, together with the power-law extrapolated TMFSS results at the corresponding phase points. The extrapolated results from the two methods agree to within the statistical uncertainty in the Monte Carlo results.

As seen in Figs. 3 and 4, there is no tricritical point for $D/|J|=1.94$, but the critical temperature goes through a minimum near $H/|J|=2$. This is the region of the phase diagram where the finite-size effects are largest, both for the Monte Carlo and transfer-matrix results. At $D/|J|=1.98$ the general shape of the phase diagram is

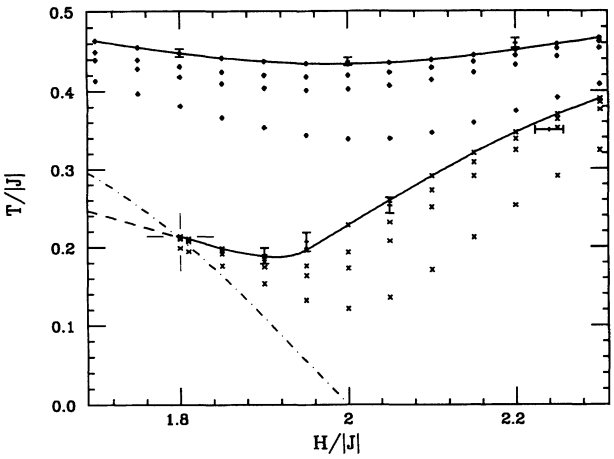

FIG. 4. Sections of the phase diagram for $D/|J|=1.94$ and 1.98, representing a close-up of Fig. 3 in the region $1.7 \leq H/|J| \leq 2.3$. The data points without error bars ($\Diamond$ for $D/|J|=1.94$ and $\times$ for 1.98) correspond (from lower to higher T) to TMFSS calculations with $M'/M=2/4$, $4/6$, and $6/8$. The solid lines are guides to the eye through the three-point power-law extrapolations to $M=\infty$, which are also marked $\Diamond$ and $\times$, respectively. The data points with error bars are L^{-1} extrapolations of Monte Carlo data for $L\times L$ systems with $L \leq 100$ for $D/|J|=1.94$ and $L \leq 200$ for $D/|J|=1.98$. As seen in Fig. 2(a) there is no tricritical point for $D/|J|=1.94$. At $D/|J|=1.98$ there is a tricritical point, whose position is indicated by the "cross hairs." The first-order line and projected tricritical line are represented by dashed and dot-dashed lines as in Fig. 3. See detailed discussion in the text.

the same as at $D/|J|=1.94$, but there is a tricritical point at $H_t/|J|=1.800\pm0.005$, $T_t/|J|=0.214\pm0.001$, as estimated from the transfer-matrix calculation with $M'/M=6/8$. This result is in agreement with the tricritical point found from Monte Carlo simulations in Ref. 12, using finite-size scaling of the order parameter, $H_t/|J|=1.77\pm0.04$, $T_t/|J|=0.22\pm0.01$. For $H<H_t$ the transition is first-order. We believe this depression in the critical temperatures near the tricritical line is caused

TABLE I. Finite-size scaling extrapolations of the critical temperature from Monte Carlo (MC) and transfer-matrix (TM) calculations. The extrapolation methods are discussed in Sec. IV for the MC case, and in Sec. III for the TM case. The TM point marked * was obtained by interpolation between two adjacent points to match the value of H obtained by the corresponding constant-temperature MC simulation. The TM results have finite-size uncertainties in the last digit.

$D/\|J\|$	$H/\|J\|$	$T_\infty/\|J\|$ (MC)	$T_\infty/\|J\|$ (TM)
1.94	1.8	0.448±0.004	0.448
1.94	2.0	0.437±0.005	0.434
1.94	2.2	0.460±0.006	0.448
1.98	1.9	0.189±0.010	0.188
1.98	1.95	0.207±0.010	0.197
1.98	2.05	0.253±0.010	0.260
1.98	2.20		0.347
1.98	2.24±0.02	0.35	0.365*
1.98	2.25		0.370

by the large fluctuations near the "missing" order-order transition, which is suppressed by the cage effect discussed in Sec. II. In all cases we find that the transition temperatures obtained from the Monte Carlo data decrease with increasing system size, whereas the transfer-matrix results increase in such a way that the transition temperature predicted by the Monte Carlo calculation always is larger than the value obtained by the transfer matrix, and such that good agreement is obtained between the extrapolated critical temperatures.

Finite-size estimates for the critical exponents ν and η were obtained as described in Sec. III and extrapolated according to Eq. (3). In the regions where the second-order transition surface is strongly curved and the finite-size effects are large, these three-point extrapolations did not converge very reliably. However, where the finite-size effects are smaller, the extrapolations converged well. For instance, at $D/|J|=1.98$ and $H/|J|=2.30$ we obtained $\nu_\infty=0.996$ and $\eta_\infty=0.249$, in excellent agreement with the exact two-dimensional Ising critical values, $\nu=1$ and $\eta=\frac{1}{4}$. Likewise, at the tricritical point for $D/|J|=1.98$ the extrapolated values were $\nu_\infty=0.536$ and $\eta_\infty=0.148$, also in very good agreement with the two-dimensional Ising tricritical values, $\nu_t=\frac{5}{9}$ and $\eta_t=\frac{3}{20}$.[47-49] A similar behavior for β was found in the Monte Carlo simulations of Ref. 12, which apply finite-size scaling to the order parameter $M_s(c)$. At $T/|J|=0.23$ and $H/|J|=0.20$, $\beta=0.13\pm0.02$, equal within statistical errors to the exact two-dimensional Ising critical value, $\beta=\frac{1}{8}$. Closer to the first-order surface, at $T/|J|=0.22$ and $H/|J|=1.77$, β decreases dramatically to 0.03 ± 0.01, in agreement within statistical errors with the tricritical value $\beta_t=\frac{1}{24}$.[47-49] The fact that near the lines where the first- and second-order surfaces join together we obtain exponents very close to the values expected for a tricritical point in a two-dimensional Ising model, we regard as further evidence that these lines are, indeed, lines of simple, two-dimensional Ising tricritical points.

VI. DISCUSSION

The purpose of this study has been to investigate the validity of the results of earlier Monte Carlo simulations,[12] which indicated that the decomposition of the tricritical line in the nearest-neighbor antiferromagnetic Blume-Capel model, which is predicted by mean-field theory[6] and has been observed by Monte Carlo simulations[11] in three dimensions, does *not* occur in two dimensions. By finite-size scaling analysis of results from numerical transfer-matrix calculations and Monte Carlo simulations, we have established that the surfaces of first- and second-order phase transitions in the two-dimensional model join smoothly, without any sign of a discontinuous change in slope, which would have been indicative of decomposition. This result is illustrated clearly in Fig. 4. At a particular point on the line where the first- and second-order surfaces join, we have also obtained estimates for the exponents ν and η from the transfer-matrix results, and β from the Monte Carlo results, which all are in close agreement with their known tricritical values for the two-dimensional Ising model. We consider that the smooth joining of the first- and second-order surfaces, together with the tricritical exponent values obtained, constitutes conclusive numerical evidence that the decomposition of the tricritical line does not take place in two dimensions, in contrast to the situation in mean-field theory and in three dimensions. This qualitative difference between mean-field theory and the behavior in three dimensions on the one hand, and the behavior in two dimensions on the other, is a consequence of the large fluctuations in the two-dimensional model, which destroy the first-order finite-temperature order-order phase transition associated with the decomposition. For the two-dimensional model with nearest-neighbor interactions these fluctuations are particularly strong, due to the cage effect discussed in Sec. II. An interesting question, which we leave for further study, is therefore whether the inclusion of weak, ferromagnetic next-nearest-neighbor interactions could reduce the fluctuations sufficiently to allow the decomposition to occur, even in two dimensions.

ACKNOWLEDGMENTS

We appreciate helpful comments from M. A. Novotny. The work was supported in part by Florida State University through its Supercomputer Computations Research Institute, which is partially funded by the U. S. Department of Energy through Contract No. DE-FC05-85ER25000, through time granted on its supercomputers, and through its Center for Materials Research and Technology. This work was also supported by The Donors of the Petroleum Research Fund, administered by the American Chemical Society, by U. S. National Science Foundation Grant No. DMR-9013107, by U. S. Department of Energy Contract No. DE-FG05-87ER40319, and by U. S. Defense Advanced Projects Agency Grant No. MDA 972-88-J-1006.

*Permanent address.

[1]M. Blume, Phys. Rev. **141**, 517 (1966).
[2]H. W. Capel, Physica **32**, 966 (1966).
[3]M. Blume, V. J. Emery, and R. B. Griffiths, Phys. Rev. A **4**, 1070 (1971).
[4]H. H. Lee and D. P. Landau, Phys. Rev. B **20**, 2893 (1979).
[5]J. B. Collins, P. A. Rikvold, and E. T. Gawlinski, Phys. Rev. B **38**, 6741 (1988).
[6]Y.-L. Wang and K. Rauchwarger, Phys. Lett. **59A**, 73 (1976).
[7]K. Motizuki, J. Phys. Soc. Jpn. **14**, 759 (1959).
[8]H. J. Herrmann, E. B. Rasmussen, and D. P. Landau, J. Appl. Phys. **53**, 7994 (1982).
[9]W. Hoston and A. N. Berker, Phys. Rev. Lett. **67**, 1027 (1991).
[10]M. Kaufman, P. E. Klunzinger, and A. Khurana, Phys. Rev. B **34**, 4766 (1986).
[11]Y.-L. Wang and J. D. Kimel, J. Appl. Phys. **69**, 6176 (1991).
[12]J. D. Kimel, S. Black, P. Carter, and Y.-L. Wang, Phys. Rev. B **35**, 3347 (1987).
[13]P. A. Rikvold, J. B. Collins, G. D. Hansen, and J. D. Gunton, Surf. Sci. **203**, 500 (1988).

[14]J. B. Colllins, P. Sacramento, P. A. Rikvold, and J. D. Gunton, Surf. Sci. **221**, 277 (1989).
[15]E. Domany, M. Schick, J. S. Walker, and R. B. Griffiths, Phys. Rev. B **18**, 2209 (1978).
[16]M. Schick, Prog. Surf. Sci. **11**, 245 (1981).
[17]Y. Saito, J. Chem. Phys. **74**, 713 (1981).
[18]M. P. Nightingale, Physica A **83**, 561 (1976).
[19]M. P. Nightingale, Phys. Lett. **59A**, 486 (1977).
[20]M. P. Nightingale, in *Finite-Size Scaling and Numerical Simulation of Statistical Systems,* edited by V. Privman (World Scientific, Singapore, 1990), p. 287.
[21]P. A. Rikvold, W. Kinzel, J. D. Gunton, and K. Kaski, Phys. Rev. B **28**, 2686 (1983).
[22]P. A. Rikvold, K. Kaski, J. D. Gunton, and M. C. Yalabik, Phys. Rev. B **29**, 6285 (1984).
[23]P. A. Rikvold, Phys. Rev. B **32**, 4756 (1985); **33**, 6523(E) (1986).
[24]N. C. Bartelt, T. L. Einstein, and L. D. Roelofs, Phys. Rev. B **34**, 1616 (1986).
[25]C. C. A. Günther, P. A. Rikvold, and M. A. Novotny, Phys. Rev. B **42**, 10 738 (1990).
[26]B. Dünweg, A. Milchev, and P. A. Rikvold, J. Chem. Phys. **94**, 3958 (1991).
[27]P. A. Rikvold, in Computer Simulation Studies in Condensed Matter Physics IV, edited by D. P. Landau, K. K. Mon, and H. B. Schüttler (Springer, Berlin, in press).
[28]T. Aukrust, M. A. Novotny, P. A. Rikvold, and D. P. Landau, Phys. Rev. B **41**, 8772 (1990).
[29]B. Derrida and L. de Seze, J. Phys. (Paris) **43**, 475 (1982).
[30]J. L. Cardy, J. Phys. A **17**, L385 (1984).
[31]V. Privman, Phys. Rev. B **32**, 6089 (1985).
[32]J. L. Cardy, in *Phase Transitions and Critical Phenomena,* edited by C. Domb and J. L. Lebowitz (Academic, London, 1987), Vol. 11.
[33]M. N. Barber, in *Phase Transitions and Critical Phenomena,* edited by C. Domb and J. L. Lebowitz (Academic, London, 1983), Vol. 8.
[34]C. J. Hamer and M. N. Barber, J. Phys. A **14**, 241 (1981).
[35]C. J. Hamer and M. N. Barber, J. Phys. A **14**, 259 (1981).
[36]C. J. Hamer and M. N. Barber, J. Phys. A **14**, 2009 (1981).
[37]N. Metropolis, A. W. Rosenbluth, A. H. Teller, and E. Teller, J. Chem. Phys. **21**, 1087 (1953).
[38]D. P. Landau, Phys. Rev. B **13**, 2997 (1975).
[39]M. E. Fisher, in *Critical Phenomena,* Proceedings of the International School of Physics "Enrico Fermi," Course 51, Varrena, Italy, 1970, edited by M. S. Green (Academic, New York, 1971).
[40]M. E. Fisher and M. N. Barber, Phys. Rev. Lett. **28**, 1516 (1972).
[41]V. Privman, in *Finite-Size Scaling and Numerical Simulation of Statistical Systems* (Ref. 20), p. 1.
[42]K. Binder, in *Finite-Size Scaling and Numerical Simulation of Statistical Systems* (Ref. 20), p. 173.
[43]D. P. Landau, in *Finite-Size Scaling and Numerical Simulation of Statistical Systems* (Ref. 20), p. 223.
[44]B. Hu, Phys. Rep. **91**, 233 (1982).
[45]H. E. Stanley, *Introduction to Phase Transitions and Critical Phenomena* (Oxford Univerisity Press, Oxford, 1971).
[46]B. M. McCoy and T. T. Wu, *The Two Dimensional Ising Model* (Harvard University Press, Cambridge, MA, 1973).
[47]M. P. M. den Nijs, J. Phys. A **12**, 1857 (1979).
[48]B. Nienhuis, E. K. Riedel, and M. Schick, J. Phys. A **13**, L189 (1980).
[49]R. B. Pearson, Phys. Rev. B **22**, 2579 (1980).